Enhanced modeling of photovoltaic modules through optimized estimation of series and shunt resistances from measured I-V curves

Ellen David Chepp^[1], Fabiano Perin Gasparin^{[2]*}, Arno Krenzinger^[3]

[1] <u>ellen.chepp@gmail.com</u>, [2] <u>fabiano.gasparin@ufrgs.br</u>, [3] <u>arno.krenzinger@ufrgs.br</u>. Universidade Federal do Rio Grande do Sul (UFRGS), Porto Alegre, Rio Grande do Sul, Brasil * autor correspondente

Abstract

The five-parameter single-diode model is widely employed to simulate the current-voltage (I-V) characteristics of photovoltaic (PV) modules. However, the estimation of series resistance (R_s) and shunt resistance (R_{sh}) from measured curves depends on the specific data ranges selected for linear regressions: in the short-circuit region for R_{sh} and in the open-circuit region for R_s . This study investigates the impact of the data range selection in the I-V curve on the analytical determination of R_s and R_{sh} . I-V curves measured under standard test conditions (STC) were used to calibrate the model, and its performance was assessed under varying irradiance and temperature levels. Differences in maximum power and RMSE of the modeled curves were analyzed. Selecting the I-V data range from zero current to 10% of the current at maximum power (IMP) for R_s , and from zero voltage to 50% of the voltage at maximum power (VMP) for R_{sh} , yielded the most accurate results, particularly under low-irradiance conditions (< 500 W/m²). Differences in modeled maximum power reached up to 12.9% when less appropriate data ranges were used. These findings contribute to a more robust modeling of PV modules under real-world operating conditions and may serve as a baseline for post-processing measured I-V curves of polycrystalline silicon PV modules to determine series and shunt resistances.

Keywords: I-V curves; modeling; photovoltaics; series resistance; shunt resistance.

Modelagem aprimorada de módulos fotovoltaicos por meio da estimativa otimizada das resistências série e shunt a partir das curvas I-V medidas

Resumo

O modelo de diodo único de cinco parâmetros é amplamente utilizado para simular as características de corrente-tensão (I-V) de módulos fotovoltaicos (FV). No entanto, a estimativa da resistência série (R_s) e da resistência shunt (R_{sh}) a partir das curvas medidas depende dos intervalos de dados específicos selecionados para regressões lineares: na região de curto-circuito para R_{sh} e na região de circuito aberto para R_s. Este estudo investiga o impacto da seleção do intervalo de dados na curva I-V na determinação gnalítica de R_s e R_{sh} . Curvas I-V medidas em condições de teste padrão (CTP) foram utilizadas para calibrar o modelo, e seu desempenho foi avaliado sob diferentes níveis de irradiância e temperatura. As diferenças na potência máxima e no RMSE das curvas modeladas foram analisadas A seleção da faixa de dados I-V de corrente zero a 10% da corrente na potência máxima (IMP) para R_s e de tensão zero a 50% da tensão na potência máxima (VMP) para R_{sh} produziu os resultados mais precisos, particularmente em condições de baixa irradiância (< 500 W/m²). As diferenças na potência máxima modelada atingiram até 12,9% quando faixas de dados menos apropriadas foram utilizadas. Esses resultados contribuem para uma modelagem mais robusta de módulos fotovoltaicos em condições operacionais reais e podem servir como base para o pósprocessamento de curvas I-V medidas de módulos fotovoltaicos de silício policristalino para determinar as resistências em série e em derivação.

Palavras-chave: curvas I-V; energia fotovoltaica; modelagem; resistência em série; resistência em derivação.

1 Introduction

Modeling I-V curves under varying irradiance and temperature conditions is essential for detailed analysis of photovoltaic (PV) module performance, both in system design and monitoring

(Ayop *et al.*, 2020; Ma *et al.*, 2020). PV modules are typically modeled using either the single-diode or the two-diode model (Humada *et al.*, 2016; Moreira *et al.*, 2021). In the case of the single-diode model, five parameters are required: series resistance (R_s), shunt resistance (R_{sh}), diode ideality factor (m), photogenerated current (IL), and diode reverse saturation current (I_0).

The determination of these five parameters can be achieved primarily through iterative methods (Villalva; Gazoli; Ruppert Filho, 2009) or analytical methods (Celik; Acikgoz, 2007; Chan; Phang, 1987). In the iterative method proposed by Villalva, Gazoli, and Ruppert Filho (2009), the value of R_s is initially set to zero and then incremented. At each increment, I_L and R_{sh} are recalculated until the estimated maximum power equals the measured maximum power. In contrast, Celik and Acikgoz (2007) and Chan and Phang (1987) proposed the calculation of initial R_s (R_{s0}) and initial R_{sh} (R_{sh0}) from the slope of the I-V curve at open-circuit and short-circuit conditions, respectively, with the remaining parameters determined through a set of analytical equations. Blas *et al.* (2002) followed a similar approach but with different simplifications.

Further improvements to analytical methods and the application of metaheuristic algorithms for parameter extraction can also be found in the literature (Arabshahi; Torkaman; Keyhani, 2020; Yang et al., 2020). Chin, Salam, and Ishaque (2015) provided a comprehensive overview of the most widely used models and extraction methods. The main advantages of analytical methods lie in their ease of implementation and accuracy of results. A drawback, however, is the requirement for the complete I-V curve of the PV module, since the calculation of R_{s0} and R_{sh0} typically relies on the slope of the measured curve. Bader, Ma, and Oelmann (2019) compared different parameter extraction methods and found that the results varied. Nevertheless, each parameter set generated an I-V curve with high accuracy, particularly at the most relevant operating points (short-circuit, open-circuit, and maximum power) under standard test conditions (STC).

When calculating R_{s0} and R_{sh0} from the slopes of the I-V curve in the open-circuit and short-circuit regions, at least two points are required, and the number of points considered influences the quality of the linear regression. Bai *et al.* (2014) calculated R_{sh0} using points from short-circuit up to the point where current equals the average between the short-circuit current and the current at maximum power. For R_{s0} , points from 50% of the current at maximum power to open circuit (0 A) were considered. Bader, Ma, and Oelmann (2019) proposed using the average of slopes calculated from different ranges of points for R_{s0} and R_{sh0} . Other studies adopted voltage ranges from 0 V to 20% of the open-circuit voltage for R_{sh0} and current ranges from 0 A to 20% of the short-circuit current for R_{s0} (Bühler; Gasparin; Krenzinger, 2014; Bühler; Krenzinger, 2013; Orioli; Di Gangi, 2013). Chan and Phang (1987), however, did not specify the number of points or ranges of current and voltage to be considered in the linear regression. Thus, while the use of specific ranges of points for calculating R_{s0} and R_{sh0} is common in the literature, the evaluation of different ranges and their impact on results has not been sufficiently addressed.

Bühler, Gasparin, and Krenzinger (2014) employed an analytical method to extract the five parameters from a measured I-V curve. Translation methods were then used to generate I-V curves under different irradiance and temperature conditions. However, such methods yield accurate results only when the range of variation in irradiance and temperature is not extensive. Bühler and Krenzinger (2013) proposed a method for extracting six parameters from the two-diode model, using I-V curves measured under STC to reproduce I-V curves under the same conditions. In practice, however, it is often necessary to model I-V curves under other environmental conditions.

In most cases, only I-V curves measured under STC are available. However, for improved reproduction of I-V characteristics, the five parameters of the single-diode model may depend on irradiance and temperature (Chegaar *et al.*, 2013; Khan; Baek; Kim, 2014). Consequently, parameters are typically determined under STC and subsequently adjusted for other conditions. Several studies have addressed the dependence of the five parameters on temperature and irradiance (Ibrahim; Anani, 2017). Ruschel, Gasparin, and Krenzinger (2021) experimentally demonstrated that R_s and R_{sh} tend to increase at low irradiance, I_L varies linearly with irradiance, and parameters m and I_0 exhibit no irradiance dependence. With respect to temperature, they found that m, R_s , and R_{sh} are unaffected, I_L varies according to the short-circuit current temperature coefficient, and I0 increases significantly with temperature. In contrast, Fébba *et al.* (2018) reported that R_s and R_{sh} are more sensitive to temperature

variations than to irradiance, showing a decreasing exponential trend with temperature and an increase in R_s with irradiance. Polverini, Tzamalis, and Müllejans (2012) concluded that variations of R_s with temperature and irradiance can be neglected, allowing R_s to be considered constant across different conditions.

Experimental studies have thus yielded divergent conclusions about the dependence of the five parameters on temperature and irradiance, particularly regarding R_s . As a result, different assumptions have been proposed for fitting parameters to model I-V curves under varying conditions. De Soto, Klein, and Beckman (2006) assumed that R_{sh} varies inversely with irradiance, R_s remains constant, and I_L varies linearly with irradiance, while both I_L and I0 depend on temperature. Similarly, Bader, Ma, and Oelmann (2019) considered I_L to vary linearly with irradiance and R_{sh} inversely with irradiance, while m, I_0 , and R_s were treated as constants. By contrast, Lo Brano $et\ al.\ (2010)$ considered both R_s and R_{sh} as inversely proportional to irradiance. Moreover, some studies did not include fitting models for the five parameters under varying conditions (Cubas; Pindado; Victoria, 2014; Villalva, Gazoli; Ruppert Filho, 2009).

In summary, the five parameters of the single-diode model are often determined from I-V curves measured under STC and subsequently adjusted for other conditions. In this approach, the choice of current and voltage ranges used in linear regression to calculate R_{s0} and R_{sh0} significantly affects the parameter determination. When parameters are further adjusted for other irradiance and temperature conditions, particularly low irradiance, differences in modeled I-V curves may arise due to the initial R_{s0} and R_{sh0} calculations. These differences and their impact on modeling accuracy have not been adequately investigated in the literature.

This article aims to address the knowledge gap regarding the most accurate method for calculating R_{s0} and R_{sh0} from an I-V curve, considering that these parameters can significantly influence the accuracy of PV modeling. Therefore, this study seeks to evaluate and optimize the calculation of R_{s0} and R_{sh0} in the single-diode model using I-V curves measured under STC. The influence of the data range considered for linear regression on both parameters is assessed to improve I-V curve modeling, particularly under low-irradiance conditions.

This article is structured as follows: Section 2 presents the detailed methodology; Section 3 discusses the main results, focusing on the optimized ranges for R_s and R_{sh} determination; and Section 4 provides the conclusions.

2 Methodology

The experimental data used in this study were obtained from the database of the Solar Energy Laboratory at the Universidate Federal do Rio Grande do Sul (Brazil), which contains I-V curves of six PV modules measured under different temperature and irradiance conditions using a solar simulator. All PV modules consist of crystalline silicon cells, and the experimental procedures are detailed by Gasparin et al. (2022).

Table 1 presents the manufacturer's specifications under standard test conditions (STC) for maximum power (P_{MP}) , voltage at maximum power (V_{MP}) , current at maximum power (IMP), open-circuit voltage (V_{OC}) , short-circuit current (I_{SC}) , number of cells in series (Ns), temperature coefficient of I_{SC} (α), and temperature coefficient of V_{OC} (β) of the PV modules analyzed in this study. The PV modules were selected based on availability and considering the significant market share of crystalline silicon modules.

Table 1 – Manufacture's specification under STC for the studied PV modules

	Module 1	Module 2	Module 3	Module 4	Module 5	Module 6
$P_{MP}\left(\mathbf{W}\right)$	290	400	260	265	400	315
$V_{MP}\left(\mathbf{V}\right)$	31.3	40.07	30.7	30.9	40.61	37.2
$I_{MP}\left(\mathbf{A}\right)$	9.25	10.02	8.48	8.61	9.85	8.48
$V_{OC}(V)$	39.3	49.39	37.8	37.9	48.93	46.2
$I_{SC}(A)$	9.8	10.42	8.99	9.11	10.36	9.01
Ns	60	72	60	60	72	72

α (%/K)	0.05	0.05	0.06	0.06	0.06	0.06
β (%/K)	-0.29	-0.27	-0.35	-0.35	-0.30	-0.31

The five parameters of the single-diode model were calculated from the I-V curves measured under STC (1000 W/m² and 25 °C) using the analytical method proposed by Chan and Phang (1987).

To calculate R_{s0} , a linear regression was performed considering the points from a defined fraction (F_y) of I_{MP} to the first point where the current became negative (I < 0). For R_{sh0} , the points from -0.3 V to a certain fraction (F_x) of V_{MP} were used. Figure 1 illustrates the range of points employed in the linear regression to calculate R_{s0} and R_{sh0} from a measured I-V curve. Several studies reported in the literature adopted data point ranges from 0 A and 0 V up to 50% of the maximum power point, or 20% of the short-circuit current and open-circuit voltage, as discussed in Section 1. In this work, both smaller and larger fractions than those commonly found in the literature were considered to verify new data range fractions.

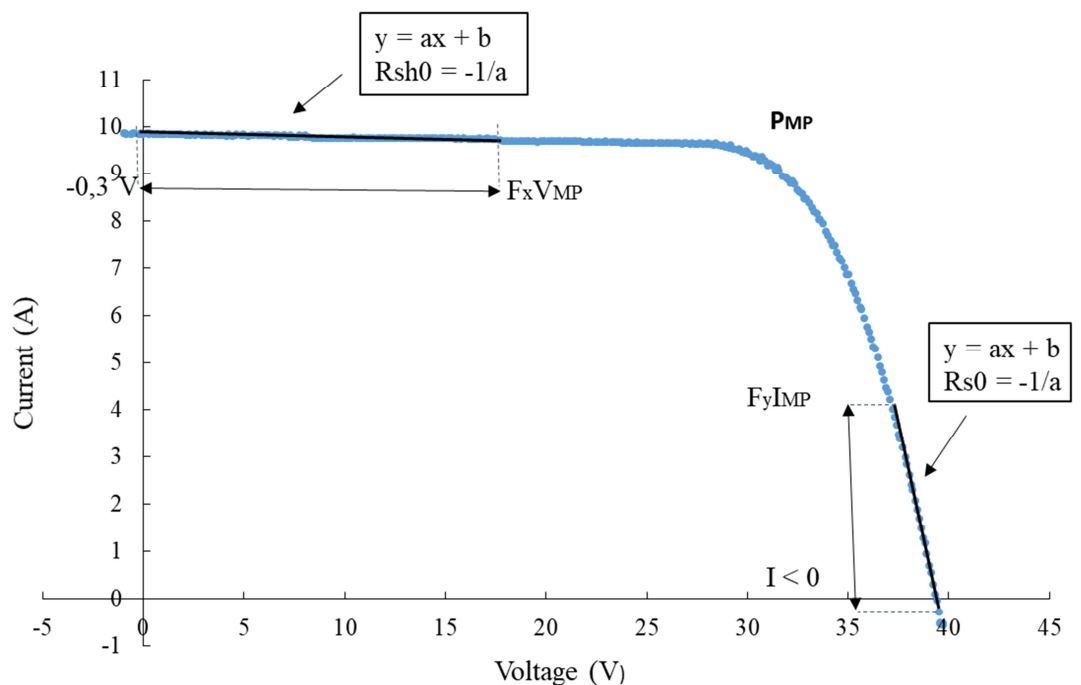


Figure 1 – Data range of a measured I-V curve considered in the calculation of R_{sh0} and R_s

Source: research data

The number of measured points considered in the regressions was defined by F_x and F_y and depended on the acquisition characteristics of the I-V tracer. The F_x and F_y values were varied to identify the most accurate resistance calculation. To analyze the effect of the selected range of points for R_{s0} , F_x was set to 0.5 for the R_{sh0} calculation, and R_{s0} was determined using different F_y values (0.1, 0.25, 0.33, 0.6, 0.7, and 0.8). Conversely, to analyze the best calculation of R_{sh0} , F_y was set to 0.1 for R_{s0} calculation, and R_{sh0} was determined using different F_x values. Therefore, six sets of five parameters of the single-diode model were determined to analyze the effects of R_{s0} , and another six to analyze the effects of R_{sh0} .

From these five parameters calculated under STC, I-V curves were modeled for other irradiance and temperature conditions. For such conditions, m and R_s were considered constant, while the remaining parameters were fitted according to Equations 1-6, where k is the Boltzmann constant (J.K⁻¹), T is the cell temperature (K), q is the electron charge (C), G is irradiance (W/m²), α is the temperature coefficient of I_{SC} (K⁻¹), and β is the temperature coefficient of V_{OC} (K⁻¹).

$$V_t = \frac{k T}{q} \tag{1}$$

$$I_{SC} = I_{SC,STC} \left(\frac{G}{1000} \right) \times (1 + \alpha (T - 298))$$
 (2)

$$V_{OC} = \left(V_{OC,STC} + mN_sV_t \ln\left(\frac{G}{1000}\right)\right) \times (1 + \beta (T - 298))$$
 (3)

$$I_L = I_{LSTC} \left(\frac{G}{1000} \right) \times (1 + \alpha (T - 298))$$
 (4)

$$R_{sh} = \frac{1000}{G} R_{sh,STC} \tag{5}$$

$$I_0 = \frac{\left(I_L - \frac{V_{OC}}{R_{sh}}\right)}{exp\left(\frac{V_{OC}}{N_s m V_t}\right) - 1} \tag{6}$$

I-V curves generated using different ranges of points defined by F_x and F_y for each irradiance and temperature condition were compared with the measured LV curves at the same conditions. Measurements were conducted with irradiance ranging from 1000 W/m² to 100 W/ m² at intervals of 100 W/ m². The cell temperature ranged from 25 °C to 65 °C in 10 °C increments. The measured I-V

curves were obtained from 353 measured points. The absolute percentage difference in maximum power between the modeled (P_P) and measured (P_M) curves was calculated according to Equation 7. The root mean square error (RMSE) of the modeled curves was also calculated, according to Equation 8, considering the number of predicted points (n), predicted values (P_i), and measured values (M_i). The best results for R_{sh0} and R_{s0} were defined based on the smallest errors.

$$Dif = \left| \frac{P_P - P_M}{P_M} \right| \times 100\% \tag{7}$$

$$Dif = \left| \frac{P_P - P_M}{P_M} \right| \times 100\%$$

$$RMSE = \sqrt{\frac{1}{n} \sum_{i=0}^{n} (P_i - M_i)^2}$$
(8)

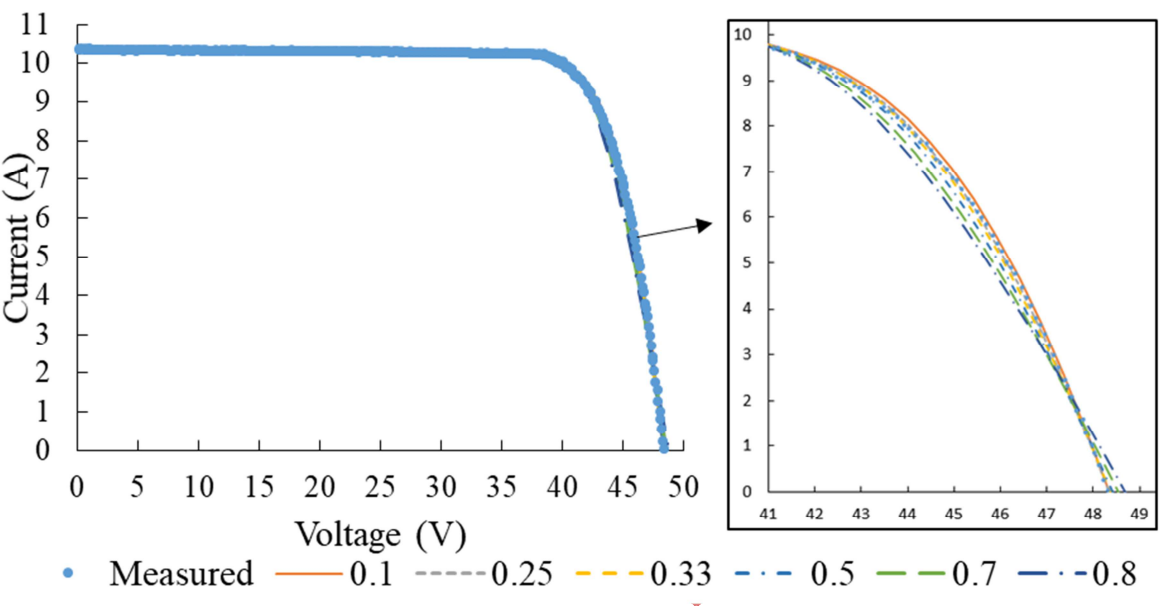
3 Results and discussion

The five parameters of the single-diode model were calculated analytically from the I-V curves measured under STC. These parameters were subsequently adjusted for other irradiance and temperature conditions, and the I-V curves were modeled accordingly.

To identify the most suitable method for determining R_{s0} , this parameter was calculated using different F_v fractions while maintaining F_x fixed at 0.5 for the calculation of R_{sh0} . I-V and P-V curves were then generated using the six sets of five parameters under varying irradiance and temperature conditions.

Figure 2 presents the measured and modeled I-V curves of PV module 5 under STC, illustrating the behavior of the modeled curves. The choice of F_v fractions in the R_{s0} calculation influenced the R_s values, which in turn affected the slope of the I-V curve near open circuit. Similar effects were observed for the other PV modules. However, the absolute differences in maximum power did not exceed 0.3%. Therefore, the variations in R_{s0} values under STC are not considered significant.

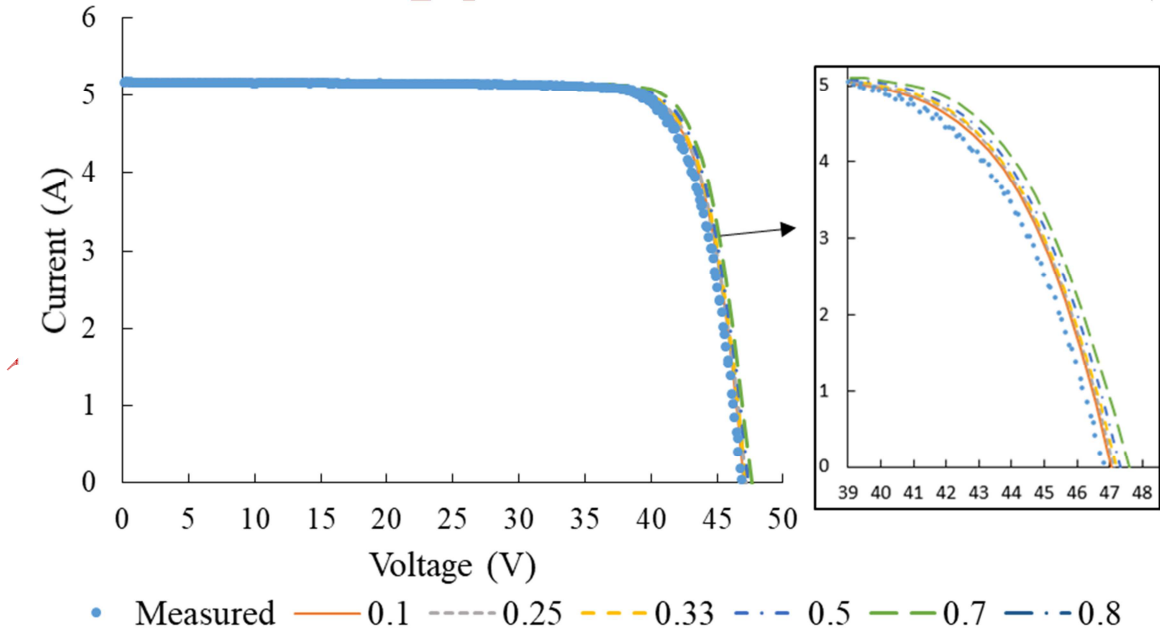
Figure 2 – Measured and modeled I-V curves of PV module 5 under STC with different F_y values for R_{s0} calculation



Source: research data

Subsequently, the five parameters were adjusted for other irradiance conditions. Figure 3 shows the I-V curves of PV module 5 at 500 W/m² and 25 °C. Differences in the modeled curves under these conditions arise from variations in R_s . In this case, the modeled curves are most accurate when Rs0 is calculated using F_v values of 0.1, 0.25, and 0.33.

Figure 3 – Modeled and measured I_z V curves of PV module 5 at 500 W/m² and 25°C with variation of F_v .



Source: research data

Figure 4 shows the I-V curves of PV module 5 at 200 W/m² and 25 °C. At lower irradiance levels, the influence of R_{s0} calculation on the I-V curves becomes more evident. The higher the F_y used in the R_{s0} calculation, the larger the discrepancies between modeled and measured curves. The most accurate results were obtained when R_{s0} was calculated with $F_y = 0.1$.

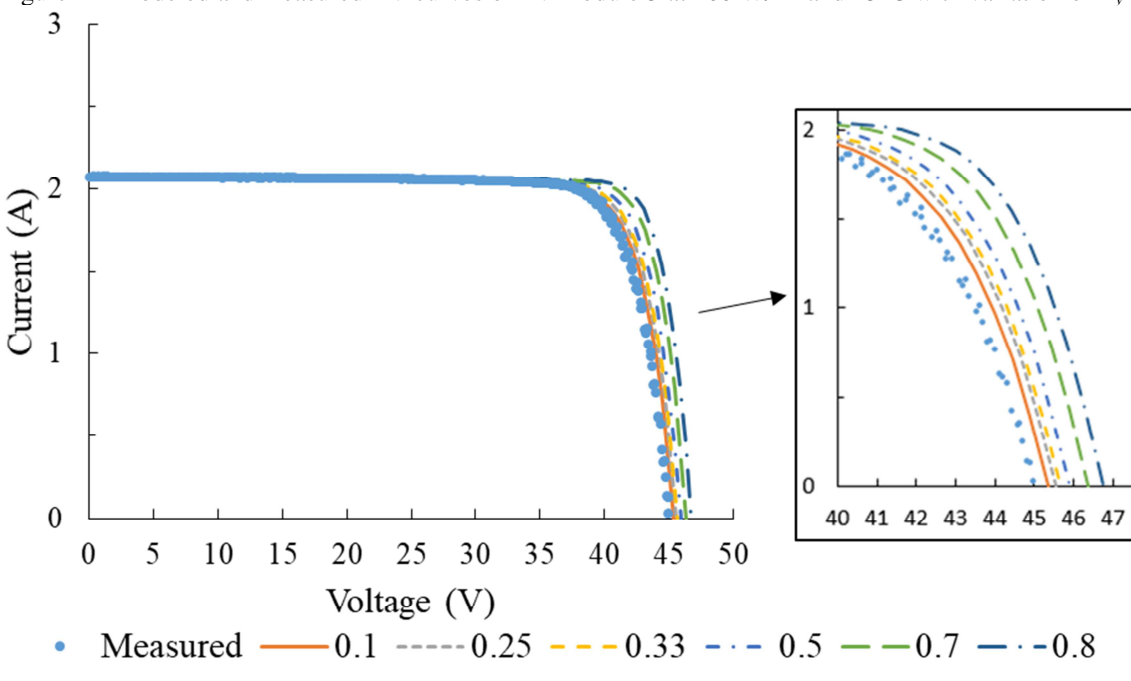


Figure 4 – Modeled and measured I-V curves of PV module 5 at 200 W/m² and 25°C with variation of F_{ν}

Source: research data

Table 2 summarizes the RMSE values of the I-V curves at 25 °C, considering all PV modules combined, under varying irradiance levels and F_y fractions. It is observed that larger F_y values lead to higher RMSE values.

Table 2 – Average RMSE of all PV	modules tested for I-V curves at $T = 25$ °C, with different F_{y} and	$\operatorname{id} G$

C (W/L-2)				$\overline{F_y}$		·
G (W/m ²)	0.1	0.25	0.33	0.5	0.7	0.8
1000	0.043435	0.038115	0.048408	0.083292	0.143126	0.180677
900	0.05114	0.041496	0.042758	0.053269	0.081277	0.10352
800	0.059419	0.05459	0.053827	0.058217	0.083401	0.110446
700	0.066875	0.069051	0.072676	0.087813	0.130063	0.168214
600	0.067092	0.078008	0.086565	0.11322	0.173291	0.222587
500	0.064091	0.081904	0.093891	0.1286	0.200708	0.256956
400	0.055266	0.077049	0.091278	0.130783	0.208808	0.267307
300	0.054106	0.077357	0.091899	0.132029	0.208262	0.263365
200	0.040579	0.062315	0.07553	0.110485	0.17273	0.214134
100	0.028025	0.041035	0.049355	0.071335	0.107315	0.127902
Mean	0.053003	0.062092	0.070619	0.096904	0.150898	0.191511

Source: research data

Table 3 presents the average differences between modeled and measured maximum power for each F_y . These differences increase with decreasing irradiance and increasing F_y . At low irradiance values, the F_y fraction used in R_{s0} calculation has a significant impact on the modeled maximum

power. For $G = 100 \text{ W/m}^2$, the discrepancies ranged from 1.1% to 12.9%. Based on the analysis of Tables 2 and 3, estimating R_{s0} with $F_y = 0.1$ yields the most accurate modeled I-V curves. The five parameters were calculated from STC curves; therefore, as irradiance decreases, the modeled curves tend to become less accurate.

Table 3 – Average differences in maximum power at T = 25°C with different F_v and G

$\frac{G \left(\text{W/m}^2 \right)}{1000}$	0.1	0.25	0.33			
1000	0.201		v.33	0.5	0.7	0.8
1000	0.2%	0.1%	0.1%	0.1%	0.2%	0.3%
900	0.3%	0.3%	0.3%	0.3%	0.4%	0.6%
800	0.4%	0.5%	0.6%	0.8%	1.3%	1.6%
700	0.5%	0.8%	0.9%	1.3%	2.0%	2.6%
600	0.7%	1.0%	1.2%	1.8%	2.9%	3.7%
500	0.7%	1.2%	1.5%	2.3%	3.7%	4.8%
400	0.6%	1.2%	1.5%	2.5%	4.4%	5.8%
300	1.1%	1.9%	2.4%	3.6%	6.1%	7.8%
200	0.8%	2.0%	2.4%	4.1%	7.2%	9.6%
100	1.1%	2.3%	2.7%	4.9%	9.5%	12.9%
Mean	0.6%	1.1%	1.4%	2.2%	3.8%	4.9%

Source: research data

Since the most accurate R_s value was obtained with the smallest analyzed fraction ($F_y = 0.1$), the five parameters were recalculated by reducing F_y to 0.05 to verify whether the R_s values would further improve the results. However, the simulated I-V curves (not shown) were less accurate under this condition compared to other fractions. Thus, $F_s = 0.1$ remains the option that provides the most accurate results.

For I-V curves at 1000 W/m² and varying temperatures, the modeled results with smaller F_y values also exhibited greater accuracy, consistent with the analysis under varying irradiance. Table 4 presents the RMSE values of the I-V curves, while Table 5 shows the maximum power error. The best results were obtained with $F_y = 0.1$, which yielded slightly lower RMSE values. Nevertheless, no significant differences were observed in P_{MP} , as indicated by the results in Table 5.

Table 4 – Average RMSF of I-V curves of six PV modules at $G = 1000 \text{ W/m}^2$ under varying T and F_v

<i>T</i> (°C)		7	F_{y}				
I(C)	0.1	0.25	0.33	0.5	0.7	0.8	
25	0.044221	0.050241	0.059073	0.090119	0.148299	0.185106	
35	0.087949	0.100832	0.104674	0.126667	0.175996	0.208782	
45	0.104503	0.113856	0.114761	0.130965	0.17591	0.207781	
55	0.147717	0.156104	0.153471	0.157205	0.182377	0.208544	
65	0.16549	0.173471	0.17301	0.179992	0.204217	0.227553	
Mean	0.109976	0.118901	0.120998	0.136989	0.17736	0.207553	

Source: research data

Table 5 – Average absolute difference at maximum power of six PV modules at $G = 1000 \text{ W/m}^2$ under varying T and F_y

<i>T</i> (°C)	F_{y}							
	0.1	0.25	0.33	0.5	0.7	0.8		
25	0.2%	0.1%	0.1%	0.1%	0.2%	0.3%		
35	0.4%	0.4%	0.4%	0.3%	0.4%	0.4%		
45	0.3%	0.3%	0.3%	0.3%	0.3%	0.3%		
55	0.8%	0.7%	0.7%	0.7%	0.7%	0.7%		

Rev. Principia, João Pessoa, e9098, 2025. Early View (será revisado e diagramado)

65	0.9%	0.9%	0.9%	0.8%	0.8%	0.8%
Mean	0.5%	0.5%	0.5%	0.5%	0.5%	0.5%

The effect of different ranges for R_{sh} calculation is illustrated in Figure 5. Significant deviations in the I-V curves of PV module 3 occurred only when $F_x = 0.1$. For all other F_x values, the modeled I-V curves closely matched the measured curve. The same effect was observed for PV module 5, as R_{sh} values calculated with $F_x = 0.1$ were significantly lower than those obtained with other fractions. The F_x parameter showed no significant effect under varying irradiance and temperature conditions. The best results were obtained with $F_x = 0.5$.

Figure 5 – Measured and modeled I-V curves of PV module 3 under STC with varying F_{x}

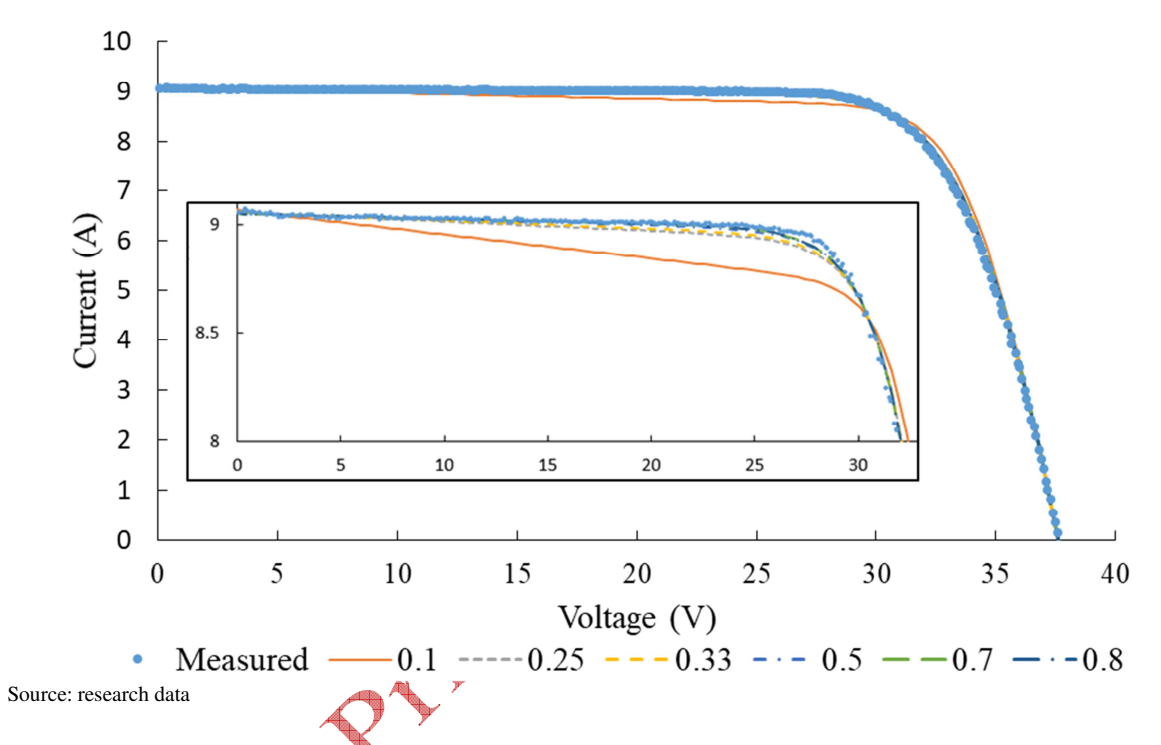


Figure 6 illustrates the influence of F_x on modeled I-V curves under low irradiance, showing that $F_x = 0.1$ can severely compromise accuracy.

Figure 6 – Modeled and measured I-V curves of PV module 3 at 200 W/m² and 25 °C with varying F_x

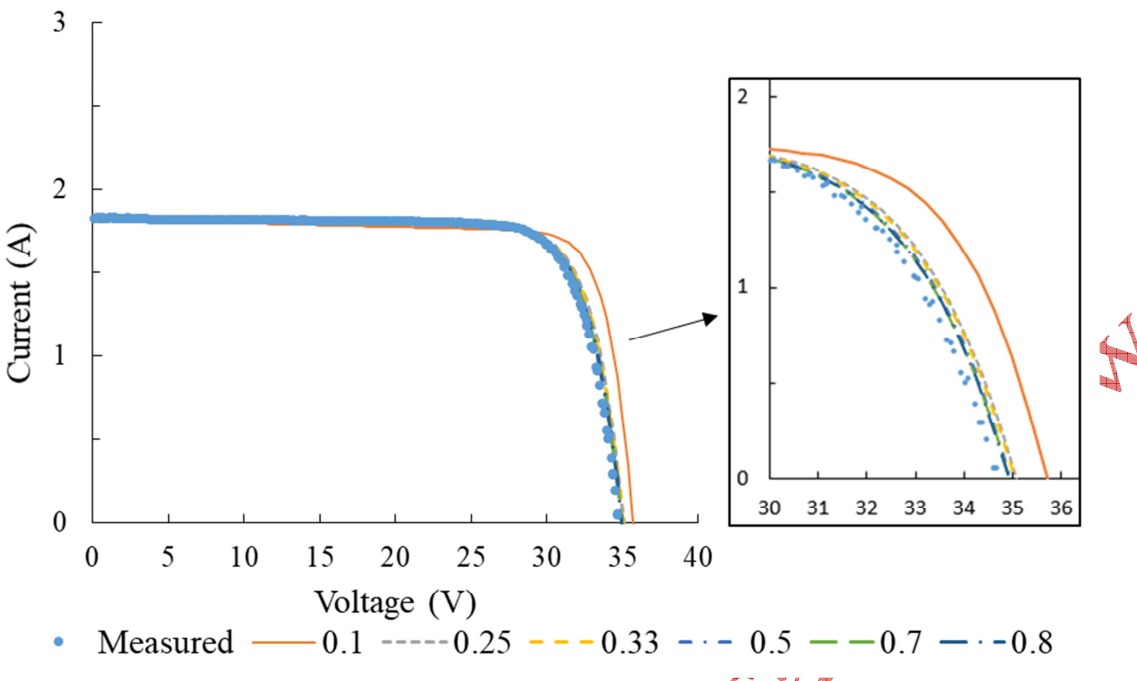


Table 6 summarizes the differences in maximum power for each PV module, considering $F_x =$ 0.1 and $F_v = 0.5$. Table 7 presents the five parameters of the single-diode model. For all PV modules, the differences tended to increase with decreasing irradiance and rising temperature. Average differences reached a maximum of 0.5% for PV modules 1, 2, 3, and 4. PV modules 5 and 6, for which the m value was lower than that of the other modules, showed average differences above 1%, with discrepancies increasing under low irradiance conditions.

Table 6 – Difference between measured and modeled maximum power for each PV module under varying T and $G(F_v = 0.1 \text{ and } F_x = 0.5)$

Condition	ons		PV Module					
G (W/m ²)	<i>T</i> (°C)	1	2	3	4	5	6	
1000	25	0.0%	0.5%	0.1%	0.1%	0.5%	0.0%	
1000	35	0.6%	0.3%	0.1%	0.5%	0.2%	0.4%	
1000	45	₩ 0.2%	0.6%	0.1%	0.1%	0.2%	0.8%	
1000	55	1.6%	0.7%	0.1%	0.3%	0.4%	1.4%	
1000	√ 65	1.7%	0.7%	0.6%	0.3%	0.4%	1.6%	
900	25	0.2%	0.2%	0.2%	0.1%	0.8%	0.2%	
800	25	0.2%	0.1%	0.5%	0.2%	1.0%	0.6%	
700	25	0.5%	0.2%	0.4%	0.1%	1.2%	0.6%	
600	25	0.5%	0.3%	0.6%	0.2%	1.4%	1.0%	
500	25	0.4%	0.3%	0.6%	0.2%	1.3%	1.4%	
400	25	0.1%	0.1%	0.2%	0.3%	1.6%	1.2%	
300	25	0.5%	0.3%	0.9%	0.4%	2.0%	2.2%	
200	25	0.1%	0.1%	0.6%	0.1%	1.7%	2.4%	
100	25	1.0%	1.0%	0.6%	0.3%	0.6%	3.3%	
Mean	1	0.5%	0.4%	0.4%	0.2%	1.0%	1.2%	

Source: research data

Table 7 – Five parameters of single-diode model calculated considering $F_v = 0.1$ and $F_x = 0.5$

PV module	R_{sh}	R_s	m	I_L	I_{θ}
1	145.3508	0.333398	1.095338	9.879054	6.89E-10
2	484.575	0.181514	1.054296	10.2346	1.48E-10
3	366.794	0.235601	1.065802	9.057612	1.00E-09
4	738.8382	0.246928	1.090776	9.112114	1.61E-09
5	508.3254	0.17157	1.004449	10.36705	5.05E-11
6	792.6312	0.316834	0.988094	9.070473	1.48E-10

The F_y value used to calculate R_{s0} from I-V curves measured under STC significantly affected the adjustment of the five parameters of the single-diode model under other irradiance conditions. However, for temperature variation, F_y did not significantly affect the modeled I-V curves under conditions other than STC. A value of $F_y = 0.1$ provided the most accurate R_s estimation, reproducing the measured I-V curves with high fidelity.

The variation of F_x had a less pronounced effect compared to F_y . For some PV modules, $F_x = 0.1$ resulted in substantially low R_{sh0} values, which reduced the accuracy of the modeled I-V curves. The most accurate results for R_{sh} determination were achieved with $F_x = 0.5$.

Previous studies analyzing the dependence of the five parameters on temperature and irradiance generally assumed fixed values of F_y and F_x for the calculation of R_{s0} and R_{sh0} . However, as demonstrated in this study, under certain conditions these fractions can significantly impact the calculated parameters of a PV module. The findings presented here indicate that assuming a constant R_s across different temperatures and irradiances is reasonable when R_{s0} is calculated with $F_y = 0.1$, whereas larger F_y values reduce accuracy. For R_{sh} determination, $F_x = 0.5$ produced the most reliable results.

4 Conclusions

This study aimed to improve the calculation of R_{s0} and R_{sh0} for the single-diode model using I-V curves of crystalline silicon PV modules measured under STC. The ranges adopted for calculating R_{s0} and R_{sh0} were defined as F_x and F_y , respectively, and the values that provided the most accurate results for modeled I-V curves were identified. To this end, the measured I-V and P-V curves of six modules under different temperature and irradiance conditions were compared with curves modeled using different F_x and F_y values.

The results indicated that $F_y = 0.1$ yielded more accurate values of R_s compared with other fractions, particularly when the five parameters of the single-diode model were adjusted for different irradiance conditions, with a greater impact observed under low irradiance. The F_x parameter had a less pronounced effect, with $F_x = 0.5$ determined as the most suitable value for R_{sh} calculation. Concerning temperature variations, both F_x and F_y showed no significant influence on the results. Using $F_x = 0.5$ and $F_y = 0.1$, the average difference between measured and estimated maximum power for all PV modules, across various irradiance and temperature levels, was 0.6%.

Therefore, the F_y value substantially affects the calculation of R_{s0} under STC and significantly impacts the results when the parameters are adjusted for other irradiance conditions. When estimating the five parameters of a PV module under STC and subsequently adjusting them to model I-V curves under different irradiance levels, it can be concluded that $F_x = 0.5$ and $F_y = 0.1$ yield the most accurate results. Furthermore, assuming a constant R_s across different temperatures and irradiances is a reasonable simplification when R_{s0} is calculated with $F_y = 0.1$.

Simulated results of PV system operation can be used for real-time monitoring to verify whether electricity generation is performing as expected, for instance. Consequently, accurate calculation of these resistances enhances monitoring reliability. The use of appropriate F_x and F_y values improves the accuracy of I-V curve modeling under low-irradiance conditions, thereby enhancing overall performance across a wide range of PV system operating conditions.

These values may also serve as reference parameters in the post-processing of I-V curves, enabling more precise analytical determination of the series and shunt resistances of PV modules. Further studies pursuing the same objective with different PV cell technologies could complement the findings discussed in this article.

Funding

This study was financed in part by Coordenação de Aperfeiçoamento de Pessoal de Nível Superior – Brazil (CAPES) – Finance Code 001 and supported by the National Council for Scientific and Technological Development (CNPq), Brazil.

Conflict of interest

The authors declare that there is no conflict of interest.

Author contributions

CHEPP, E. D.: conception or design of the study/research; data collection, analysis, and/or interpretation; preparation and writing of the manuscript. GASPARIN, F. P.: conception or design of the study/research; preparation and writing of the manuscript; critical review, with significant intellectual participation. KRENZINGER, A.: conception or design of the study/research; critical review, with significant intellectual participation; general supervision and coordination of the project or study. All authors participated in the writing, discussion, reading and approval of the final version of the article.

References

ARABSHAHI, M. R.; TORKAMAN, H.; KEYHANI, A. Amethod for hybrid extraction of single-diode model parameters of photovoltaics. **Renewable Energy**, v. 158, p. 236-252, 2020. DOI: https://doi.org/10.1016/j.renene.2020.05.035.

AYOP, R.; TAN, C. W.; MAHMUD, M. S. A.; NASIR, S. N. S.; AL-HADHRAMI, T.; BUKAR, A. L. A simplified and fast computing photovoltaic model for string simulation under partial shading condition. **Sustainable Energy Technologies and Assessments**, v. 42, e100812, 2020. DOI: https://doi.org/10.1016/j.seta.2020.100812.

BADER, S.; MA, X.; OELMANN, B. One-diode photovoltaic model parameters at indoor illumination levels: a comparison. **Solar Energy**, v. 180, p. 707-716, 2019. DOI: https://doi.org/10.1016/j.solener.2019.01.048.

BAI, J.; LIU, S.; HAO, Y.; ZHANG, Z.; JIANG, M.; ZHANG, Y. Development of a new compound method to extract the five parameters of PV modules. **Energy Conversion and Management**, v. 79, p. 294-303, 2014. DOI: https://doi.org/10.1016/j.enconman.2013.12.041.

BLAS, M. A.; TORRES, J. L.; PRIETO, E.; GARCÍA, A. Selecting a suitable model for characterizing photovoltaic devices. **Renewable Energy**, v. 25, n. 3, p. 371-380, 2002. DOI: http://doi.org/10.1016/S0960-1481(01)00056-8.

BÜHLER, A. J.; GASPARIN, F. P.; KRENZINGER, A. Post-processing data of measured I-V curves of photovoltaic devices. **Renewable Energy**, v. 68, p. 602-610, 2014. DOI: https://doi.org/10.1016/j.renene.2014.02.048.

BÜHLER, A. J.; KRENZINGER, A. Method for photovoltaic parameter extraction according to a modified double-diode model. **Progress in Photovoltaics: Research and Applications**, v. 21, n. 5, p. 884-893, 2013. DOI: https://doi.org/10.1002/pip.2170.

- CELIK, A. N.; ACIKGOZ, N. Modelling and experimental verification of the operating current of mono-crystalline photovoltaic modules using four- and five-parameter models. **Applied Energy**, v. 84, n. 1, p. 1-15, 2007. DOI: https://doi.org/10.1016/j.apenergy.2006.04.007.
- CHAN, D. S. H.; PHANG, J. C. H. Analytical methods for the extraction of solar-cell single- and double-diode model parameters from I-V characteristics. **IEEE Transactions on Electron Devices**, v. 34, n. 2, p. 286-293, 1987. DOI: https://doi.org/10.1109/T-ED.1987.22920.
- CHEGAAR, M., HAMZAOUI, A., NAMODA, A., PETIT, P., AILLERIE, M., HERGUTH, A. Effect of illumination intensity on solar cells parameters. **Energy Procedia**, v. 36, p. 722-729, 2013. DOI: https://doi.org/10.1016/j.egypro.2013.07.084.
- CHIN, V. J.; SALAM, Z.; ISHAQUE, K. Cell modelling and model parameters estimation techniques for photovoltaic simulator application: a review. **Applied Energy**, v. 154, p. 500-519, 2015. DOI: https://doi.org/10.1016/j.apenergy.2015.05.035.
- CUBAS, J.; PINDADO, S.; VICTORIA, M. On the analytical approach for modeling photovoltaic systems behavior. **Journal of Power Sources**, v. 247, p. 467-474, 2014. DOI: https://doi.org/10.1016/j.jpowsour.2013.09.008.
- DE SOTO, W.; KLEIN, S. A.; BECKMAN, W. A. A. Improvement and validation of a model for photovoltaic array performance. **Solar Energy**, v. 80, n. 1, p. 78-88, 2006. DOI: https://doi.org/10.1016/j.solener.2005.06.010.
- FÉBBA, D. M.; RUBINGER, R. M.; OLIVEIRA, A. F.; BORTONI, E. C. Impacts of temperature and irradiance on polycrystalline silicon solar cells parameters. **Solar Energy**, v. 174, p. 628-639, 2018. DOI: https://doi.org/10.1016/j.solener.2018.09.051
- GASPARIN, F. P.; KIPPER, F. D.: OLIVEIRA, F. S.; KRENZINGER, A. Assessment on the variation of temperature coefficients of photovoltaic modules with solar irradiance. **Solar Energy**, v. 244, p. 126-133, 2022. DOI: https://dx.org/10.1016/j.solener.2022.08.052.
- HUMADA, A. M.; HOJABRI, M.; MEKHILEF, S.; HAMADA, H. M. Solar cell parameters extraction based on single and double-diode models: a review. **Renewable and Sustainable Energy Reviews**, v. 56, p. 494-509, 2016. DOI: https://doi.org/10.1016/j.rser.2015.11.051.
- IBRAHIM, H.; ANANI, N. Variations of PV module parameters with irradiance and temperature. **Energy Procedia**, v. 134, p. 276-285, 2017. DOI: https://doi.org/10.1016/j.egypro.2017.09.617.
- KHAN, F.; BAEK, S.-H.; KIM, J. H. Intensity dependency of photovoltaic cell parameters under high illumination conditions: an analysis. **Applied Energy**, v. 133, p. 356-362, 2014. DOI: https://doi.org/10.1016/j.apenergy.2014.07.107.
- LO BRANO, V.; ORIOLI, A.; CIULLA, G.; DI GANGI, A. An improved five-parameter model for photovoltaic modules. **Solar Energy Materials and Solar Cells**, v. 94, n. 8, p. 1358-1370, 2010. DOI: https://doi.org/10.1016/j.solmat.2010.04.003.
- MA, M.; ZHANG, Z.; XIE, Z.; YUN, P.; ZHANG, X.; LI, F. Fault diagnosis of cracks in crystalline silicon photovoltaic modules through I-V curve. **Microelectronics Reliability**, v. 114, e113848, 2020. DOI: https://doi.org/10.1016/j.microrel.2020.113848.
- MOREIRA, H. S.; SILVA, J. L. S.; REIS, M.V. G.; MESQUITA, D. B.; PAULA, B. H. K.; VILLALVA, M. G. Experimental comparative study of photovoltaic models for uniform and partially

shading conditions. **Renewable Energy**, v. 164, p. 58-73, 2021. DOI: https://doi.org/10.1016/j.renene.2020.08.086.

ORIOLI, A.; DI GANGI, A. A procedure to calculate the five-parameter model of crystalline silicon photovoltaic modules on the basis of the tabular performance data. **Applied Energy**, v. 102, p. 1160-1177, 2013. DOI: https://doi.org/10.1016/j.apenergy.2012.06.036.

POLVERINI, D.; TZAMALIS, G.; MÜLLEJANS, H. A validation study of photovoltaic module series resistance determination under various operating conditions according to IEC 60891. **Progress in Photovoltaics: Research and Applications**, v. 20, n. 6, p. 650-660, 2012. DOI: https://doi.org/10.1002/pip.1200.

RUSCHEL, C. S.; GASPARIN, F. P.; KRENZINGER, A. Experimental analysis of the single diode model parameters dependence on irradiance and temperature. **Solar Energy**, v. 217, p. 134-144, 2021. DOI: https://doi.org/10.1016/j.solener.2021.01.067.

VILLALVA, M. G.; GAZOLI, J. R.; RUPPERT FILHO, E. Modeling and circuit-based simulation of photovoltaic arrays. *In*: 2009 BRAZILIAN POWER ELECTRONICS CONFERENCE (COBEP), 2009, Bonito. **Proceedings** [...]. Bonito: IEEE, 2009. DOI: https://doi.org/10.1109/COBEP.2009.5347680.

YANG, B.; WANG, J.; ZHANG, X.; YU, T.; YAO, W.; SHU, R.; ZENG, F.; SUN, L. Comprehensive overview of meta-heuristic algorithm applications on PV cell parameter identification. Energy Conversion and Management, v. 208, e112595, 2020. DOP: https://doi.org/10.1016/j.enconman.2020.112595.